NUKLEONIKA 2024;69(2):135–140
doi: 10.2478/nuka-2024-0020

ORIGINAL PAPER

Conversion of fast neutrons for neutron radiography with TPX2 detector

Andrea Šagátová,
Marko Fülöp,
Andrej Novák,
Branislav Vrban,
Jakub Lüley,
Štefan Čerba,
Ivan Benkovský,
Bohumír Zaťko

Abstract. The Timepix2-based hybrid-pixel detector with a 500 μm thick silicon sensor was employed for fast-neutrons registration to be applied in neutron radiography of metallic printed circuit heat exchanger (PCHE). Two energies of neutrons were experimentally tested. The detection of 3.55 MeV neutrons from the deuteron–deuteron (DD) reaction was compared to 15.7 MeV neutrons from the deuteron–tritium (DT) neutron generator. In order to distinguish the signal induced by the registered neutrons from the accelerator background, filtration of the recorded particle spectral tracks was applied. The benefit of applying hydrogen-based converter layer for 3.55 MeV neutrons was observable. On the other hand, in the case of 15.7 MeV neutrons, the direct registration by interaction with the sensor Si significantly dominates the conversion.

Keywords: Hybrid pixel detector • Neutron conversion • Neutron radiography • Timepix2

A. Šagátová✉, A. Novák, B. Vrban, J. Lüley, Š. Čerba
Slovak University of Technology in Bratislava
Institute of Nuclear and Physical Engineering
Faculty of Electrical Engineering and Information Technology
Ilkovičova 3 St., 841 04 Bratislava, Slovak Republic
E-mail: andrea.sagatova@stuba.sk

M. Fülöp
ABRS Ltd.
Pomlejská 106 St., 931 01 Šamorín, Slovak Republic

I. Benkovský
Comenius University in Bratislava
Faculty of Pharmacy
Odbojárov 10 St., 832 32 Bratislava, Slovak Republic

B. Zaťko
Slovak Academy of Sciences
Institute of Electrical Engineering
Dúbravská cesta 9 St., 841 01 Bratislava, Slovak Republic

Received: 21 November 2023
Accepted: 8 May 2024

Introduction

The non-destructive analysis [1] is an important technique for the inspection of critical components in the industry, such as the new class of compact heat exchangers, the printed circuit heat exchanger (PCHE) applicable in Generation IV nuclear reactors or solar power plants. The PCHE behaves as a single metal block, with etched holes running through it, withstanding high-pressure differences between the primary and the secondary coolant sides accompanied by compact size and high thermal efficiency, up to 98% [2, 3]. To reduce the time and cost associated with the maintenance tasks of future energy systems, engineers need to quickly identify the potential defects by non-destructive techniques. Due to the metal composition of the PCHE, fast-neutron radiography is the most suitable technique.

A new concept of neutron digital radiography with fast neutrons produced by a deuteron–deuteron (DD) neutron generator and a Timepix-based detector is planned to be used for PCHE examination. The neutrons will be produced by the $D(d,n)^3He$ nuclear reaction ($Q = 3.269$ MeV) [4], with neutron energies in the range of 2–5 MeV depending on the initial deuteron beam energy. For neutron registration, the MiniPIX TPX2 detector [5] with a 500 μm thick silicon sensor was chosen. In order to improve the detection efficiency of the TPX2 detector, conversion layers were applied on the sensor surface, to exploit the elastic scattering of neutrons on hydrogen. The effect of the conversion layers on the registration of two types of fast neutrons, the 3.55 MeV and 15.7 MeV, was evaluated.

MiniPIX TPX2 detector

The MiniPIX TPX2 detector is a hybrid semiconductor multi-pixel detector of the Timepix family designed by Advacam [5]. The Timepix type detectors utilize the readout electronics integrated on an ASIC chip [6–8] to evaluate the signal measured by a pixelated semiconductor sensor registering single particles of ionizing radiation. The sensor is typically made of Si (silicon), nevertheless, also other semiconductor materials are being used, e.g. CdTe, GaAs, or recently also SiC [9–13]. The MiniPIX TPX2 detector is prepared by bump-bonding a pixelated sensor to a Timepix2 readout ASIC chip [8], with a matrix of 256 × 256 pixels with 55 μm pitch covering an area of 1.4 cm × 1.4 cm. The sensor of the used TPX2 detector was made of 500 μm thick silicon with each of its 65 536 pixels representing an independent detecting unit (Fig. 1). Previous detectors of the Timepix type, the Timepix, and the Timepix3, have already been tested for the detection of fast neutrons [14–16], partially enhancing the detection efficiency using a hydrogen-based converter layer. The problem of semiconductor detectors for neutron detection is that they are sensitive to all types of ionizing radiation and in mixed radiation fields like around neutron sources, the signal from neutrons is overlapped by other unwanted radiation types, mainly the X- and gamma rays. On the other hand, the pixelization of the sensor is sufficiently small regarding the particle track (the charge cloud produced during particle interaction in the sensor) and the track usually overlaps a group of pixels creating the pixel cluster. Consequently, the hybrid pixel detector registers single particles with their tracks with attribution of energy loss in the sensor at each point of the track, with pixel spatial resolution, the so-called spectral track. One can utilize the track analysis to recognize the neutron product tracks from other registered particles as each type of radiation differs in track shape and energy released [17]. The idea of utilizing the pattern recognition algorithms on the spectral tracks of registered particles was introduced by Granja *et al.* [16] to decompose the neutron-induced tracks into particle event types, when measuring the 2.6 MeV and 14.1 MeV neutrons by the Timepix3 detector with 500 μm Si sensor.

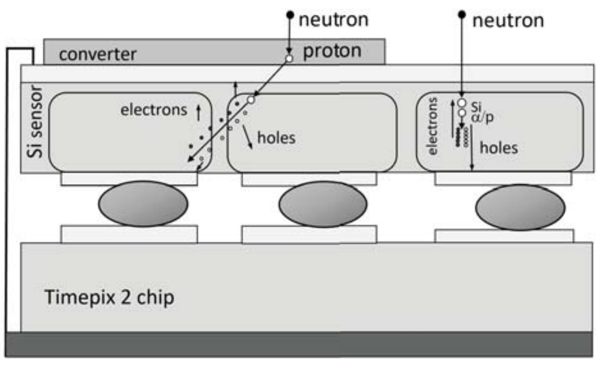

Fig. 1. Schematic cross-section view of TPX2 chip bump-bonded to Si sensor with examples of neutron registration: through conversion in polyethylene (left) or by nuclear reaction with Si nucleus (right).

The MiniPIX TPX2 detector utilizes the latest Timepix readout ASIC chip, the Timepix2. The chip provides fast frame-based readout, a wide spectral range for each pixel up to a few MeV, and a new function “the first-hit of pixel” registering only the track of the particle that first hits the pixel, preventing from summing multiple tracks into one. All these characteristics make the Timepix2 detector ideal for utilizing track filtration to recognize registered neutrons in mixed radiation fields.

The TPX2 detector was enhanced for the registration of fast neutrons by converter layers with hydrogen to register neutrons through elastic scattering on hydrogen nuclei. To compare the effect of various conversion layers, the parts of the sensor surface were coated by different layers as shown in Fig. 2. The left part shows the photograph of the MiniPIX TPX2 detector with the applied layers. The middle part shows an X-ray image of the applied layers, precisely defining the position of the layer over certain pixels and the right image shows the areas of the sensor covered by converter layers in color: #0 without any layer, #1 Kapton polyimide film (10 μm thick), #2, #3, #4 polyethylene (PE) layers: 50 μm, 100 μm, and 150 μm thick.

Experiment

The quality of the TPX2 detector in registering the neutrons from the neutron generator was examined at the Van de Graaff laboratory of the Institute of Experimental and Applied Physics CTU in Prague. Two different MeV energies of neutrons were compared, the neutrons from DD and DT nuclear reactions, respectively:

(1) $$\mathrm{D} + \mathrm{D} \rightarrow {}^{3}\mathrm{He}\ (0.82\ \mathrm{MeV}) + \mathrm{n}\ (2.45\ \mathrm{MeV})$$

(2) $$\mathrm{D} + \mathrm{T} \rightarrow {}^{4}\mathrm{He}\ (3.52\ \mathrm{MeV}) + \mathrm{n}\ (14.06\ \mathrm{MeV})$$

During the first experiment, the TPX2 detector was placed at an angle of 50° in front of the deuterium target impinged by the deuterons accelerated to energy of 1 MeV/A. The energy of neutrons hitting the detector was 3.55 MeV [4]. During the second experiment, the target was exchanged for a tritium one and was bombarded by 0.85 MeV/A deuterons. The energy of the released neutrons <50° was 15.7 MeV [4]. The photograph of the experimental setup is shown in Fig. 3.

The TPX2 detector with Si sensor registers fast neutrons either directly through reactions on Si or indirectly utilizing converter layers. More than 92% of naturally occurring Si is created by the ^{28}Si isotope. The neutrons can interact with the ^{28}Si in the sensor by elastic scattering or by several nuclear reactions, which are energy limited by their Q value.

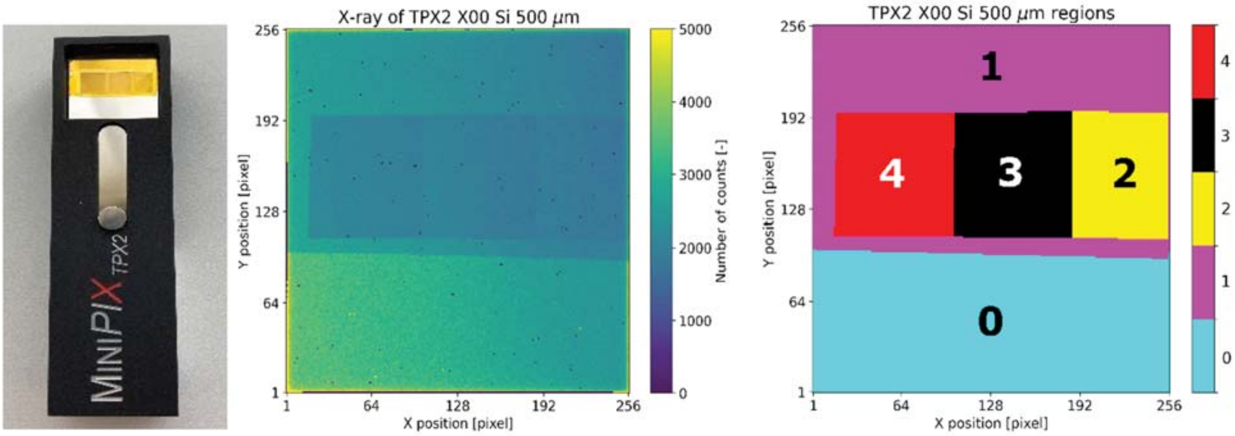

Fig. 2. The photograph of the MiniPIX TPX2 detector with applied layers (left). The X-ray image of the layers applied on the sensor substrate (middle). Areas of the sensor covered by different converter layers in color (right).

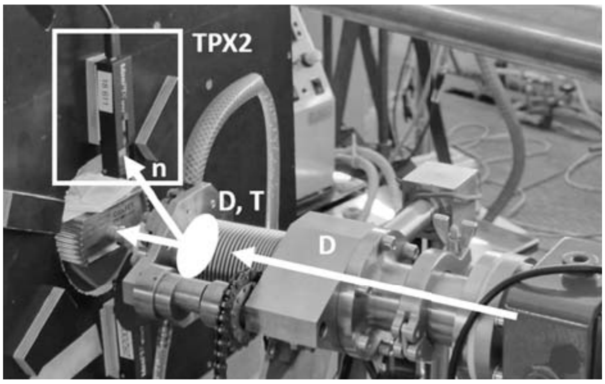

Fig. 3. Arrangement of experimental testing of the TPX2 detector by fast neutrons.

Some of the possible reactions are listed in Table 1 together with their calculated Q values. More reactions can be found elsewhere [18, 19]. In the case of our experiment with 3.55 MeV neutrons, only the elastic scattering (n,n), radiative capture (n,γ) and (n,α) nuclear reactions were possible. With 15.7 MeV, more reaction channels are opened, including the (n,p) nuclear reaction. The electrically charged products of the interactions transfer their energy into the sensor by ionization of atoms, thus indirectly registering neutrons. The reaction products, the protons, alpha particles, or heavy ions, gradually ionize Si atoms forming a charge cloud on a short trajectory in the shape of a circle extending over several pixels in the sensor. Particles with higher energy will produce a larger cloud, the circle track will be spread over more pixels. The energetic per pixel calibration of the TPX2 detector enables to determine the released energy in the particle track, in other words in the cluster of active pixels. The total kinetic energy of the reaction products for both energies of the interacting neutrons is listed in Table 1. The trajectories of particles from the accelerator background, from gamma rays or beta particles, differ from the shape and the released energy of neutron recoils [20], enabling their filtration.

The converter layers covering the TPX2 detector common electrode were used to convert the neutrons into ionizing particles directly registerable by the detector. The PE layers of 50 μm, 100 μm, and 150 μm thickness were fixed by the 10 μm Kapton polyimide film, where neutrons elastically scatter on hydrogen. Table 2 shows the projected ranges of scattered protons of maximum energy in the converter layers used.

Table 1. Selected interactions of fast neutrons in Si sensor and conversion layer with their Q values and total energy of recoils for interacting neutrons with kinetic energy of 3.55 MeV and 15.7 MeV with parameters for elastic scattering on hydrogen in the converter layer

Interaction	Q value (MeV)	Total kinetic energy of charged recoils (MeV)	
		@ 3.55 MeV neutrons	@ 15.7 MeV neutrons
$^{28}Si(n,n')^{28}Si$ (elastic sc.)	0	up to 0.47	up to 2.09
$^{28}Si(n,n')^{28}Si^{*}$	–1.779	1.771	13.921
$^{28}Si(n,\alpha)^{25}Mg$	–2.654	0.896	13.046
$^{28}Si(n,\alpha)^{25}Mg^{*}$	–3.239	0.311	12.461
$^{28}Si(n,\alpha)^{25}Mg^{**}$	–3.628	–	12.072
$^{28}Si(n,\alpha)^{25}Mg^{***}$	–4.266	–	11.434
$^{28}Si(n,\alpha)^{25}Mg^{****}$	–4.618	–	11.082
$^{28}Si(n,\alpha)^{25}Mg^{*****}$	–5.455	–	10.245
$^{28}Si(n,\alpha)^{25}Mg^{******}$	–6.059	–	9.641
$^{28}Si(n,p)^{28}Al$	–3.860	–	11.840
$^{28}Si(n,d)^{27}Al$	–9.360	–	6.340
$^{28}Si(n,\gamma)^{29}Si$	8.474	12.024	24.174
H(n,p)n	0	up to 3.55	up to 15.7

*The first excited state of the nucleus, up to ****** 6th excited state of the nucleus.

Table 2. Projected ranges of protons in converter layers applied on the sensor surface according to SRIM [21]

Proton energy (MeV)	Kapton polyimide film $C_{22}H_{10}N_2O_5$ (1.42 g/cm^3, 10 μm)	Polyethylene $(C_2H_4)_n$ (0.93 g/cm^3, 50–150 μm)
	Projected range (μm)	
3.55	152.24	190
15.70	2090	2700

Results and discussion

The tracks of the first 2000 particles registered by the TPX2 detector with filtration applied to distinguish the signal of the neutrons from the gamma and the electron background are depicted in Fig. 4. Protons, alphas, and heavy ions from neutron interactions have expected energy >0.5 MeV (Table 1) and round tracks with size S >20 pixels. Various conditions for roundness from >0.5 (mixed field), through >0.9, up to >0.99 (well-filtered alphas, protons, and recoils with almost ideal circle shape (circle has roundness = 1)) in the first up to the third row of Fig. 4 are depicted for 3.55 MeV and 15.7 MeV neutrons in two columns.

The filtration of registered particle tracks was done utilizing the data processing engine (DPE) [22] developed by Advacam [5] and the Python programming language [23]. The DPE is a software which enables per-pixel calibration of the Timepix detector and calculation of various parameters of particle tracks, the clusters of activated pixels. The DPE gives a set of about 20 raw data for each particle track: e.g., cluster size, total energy, the highest per pixel energy of cluster, roundness, its position in the pixel field, border pixel count, linear energy transfer (LET), which can be used to distinguish the tracks based on the nature of particle interaction.

One can observe that the 3.55 MeV neutron-induced tracks are well-distinguished below the

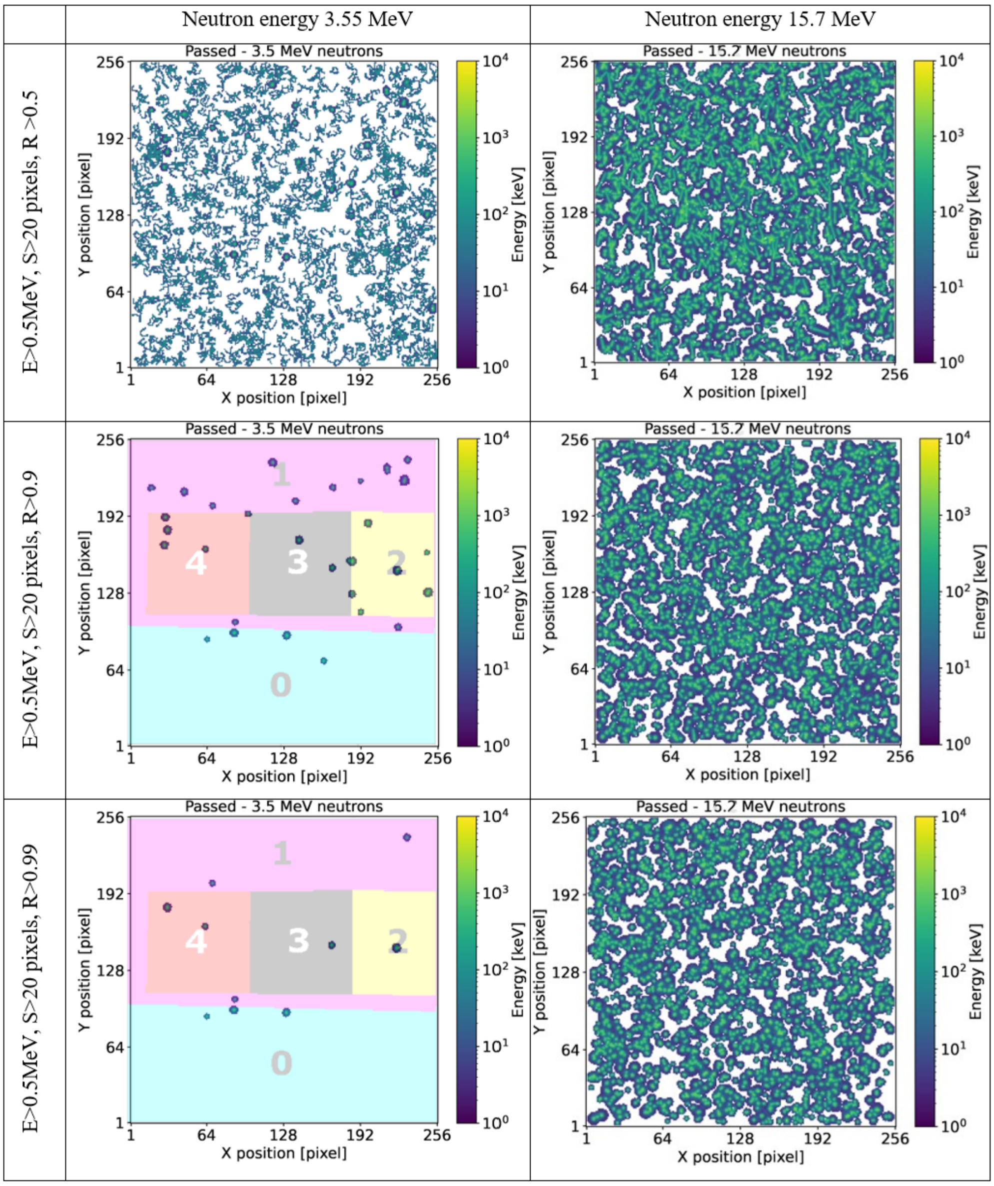

Fig. 4. Tracks of the first 2000 particles registered by the TPX2 detector with applied filtration are described in the left column for two energies of interacting neutrons: 3.55 MeV (middle column) and 15.7 MeV (right column).

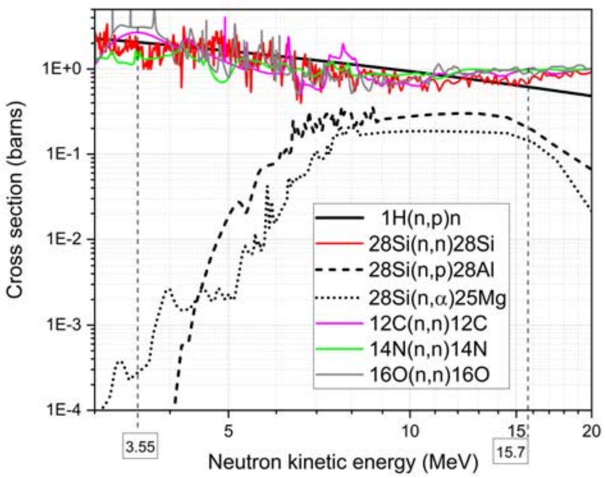

Fig. 5. The cross-sections of selected reactions on ^{28}Si and elastic scattering on ^{1}H, ^{12}C, ^{14}N, and ^{16}O as a function of neutron kinetic energy obtained from ENDF/B-VII.1 [24].

converter layers, and in the case of 15.7 MeV neutrons, the tracks are distributed through the whole sensor. This can be explained by the probability of neutron interactions. The most probable are elastic scatterings on converter layers' atoms and Si for MeV energies of interacting neutrons (Fig. 5). In the case of 3.55 MeV neutrons, the elastic scattering on atoms' nuclei in converter layers dominates with about 2 barns cross-section over (n,α) nuclear reaction in the sensor (3×10^{-4} barns). The elastic scattering on Si (2 barns), however, produces charged ^{28}Si ions with energy <0.5 MeV, which tracks do not pass the filter. That is why the tracks occur in the area of the applied converter layers, where the recoils are lighter and gain a larger part of energy than Si during elastic scattering. In the case of 15.7 MeV neutrons all interactions, the elastic scattering in the converter layer or Si as well as the nuclear reactions on Si, have a similar order of cross-section. However, the volume of the Si (with 500 μm thickness) exceeds the volume of the converter layers (10–150 μm thick), which explains why the tracks of the neutron interaction products can be seen all over the area of the sensor, regardless the position of the converter layers.

The analysis of raw data from the experiment with 3.55 MeV neutrons shows 571 842 separated tracks during 280 s, where from the first 2000 tracks only those are depicted in Fig. 4, which passed the filter defined on the left (energy >500 keV, number of pixels in cluster >20 and roundness) supposed to be the heavily charged particle tracks, tracks of the products of neutron interaction (protons, alphas, and recoils). In the case of the filter with roundness >0.9, it is 30 tracks, dominantly under converter layers and Kapton film. The neutron flux on the detector was 2700/s/cm^2. The dominant effect of Kapton film can be observed and it was calculated that it increased the detection efficiency from the initial 0.04 ± 0.03% (bare detector) to 0.4 ± 0.2% (with converter layer) regardless of the PE layer presence. The Kapton film density exceeds the density of PE.

Conclusions

For neutron radiography of PCHE for nuclear reactors of Generation IV, the quasi-monoenergetic neutrons produced via the D(d,n)^{3}He nuclear reaction (Q = 3.269 MeV) with energies in the range of 2–5 MeV depending on the initial beam energy are planned to be used. The neutrons will be registered by the Timepix2 detector with a 500 μm thick Si sensor after penetration of the PCHE experimental model. To enhance the detection efficiency of the Timepix2 silicon detector in this energy range, the Kapton film would be beneficial, when the recoils from elastic scattering of neutrons in the film dominate the signal from direct registration of neutrons on Si atoms. The effect of the PE converter layer on the detection efficiency of neutrons was not confirmed by the experiment.

Acknowledgment. This study has been financially supported by FEEIT STU through the project NERAKO. This project has received funding from the European Union's Horizon 2020 Research and Innovation Programme under GA no. 101004730 and from the Slovak Research and Development Agency under grant no. APVV-22-0382. The neutron fields used for the measurements were provided in the open-access regime by the Van de Graaff accelerator facility of IEAP CTU in Prague, whose operation was supported by the Research Infrastructure Grant LM2018108 of the Ministry of Education, Youth and Sports of the Czech Republic.

ORCID

Š. Čerba http://orcid.org/0000-0002-4065-3976
J. Lüley http://orcid.org/0000-0001-9702-2895
A. Novák http://orcid.org/0000-0003-3308-7256
A. Šagátová http://orcid.org/0000-0002-8519-7206
B. Vrban http://orcid.org/0000-0002-8951-0052
B. Zaťko http://orcid.org/0000-0003-0612-6264

References

1. International Atomic Energy Agency. (2013). *Training guidelines in non-destructive testing techniques*. Vienna: IAEA.
2. Chang, C. Y., Che, W. H., Saw, L. H., & Arpia, A. A. (2021). Performance analysis of a printedcircuit heat exchanger with a novel mirror-symmetric channel design. *Energies*, *14*(14), 4252. https://doi.org/10.3390/en14144252.
3. Aakre, S. (2018). Nuclear code case development of printed-circuit heat exchangers with thermal and mechanical performance testing. In 6th International Supercritical CO_2 Power Cycles Symposium, Pittsburgh.
4. Liskien, H., & Paulsen, A. (1973). Neutron production cross sections and energies for the reactions T(p,n)^{3}He, D(d,n)^{3}He, and T(d,n)^{4}He. *Atom. Data Nucl. Data Tabl.*, *11*(7), 569–619. DOI: 10.1016/S0092-640X(73)80081-6.

5. Advacam. (2023, November). *MiniPIX TPX2*. Retrieved November 13, 2023, from https://advacam.com/camera/minipix-tpx2/.
6. Llopart, X., Ballabriga, R., Campbell, M., Tlustos, L., & Wong, W. (2007). Timepix, a 65k programmable pixel readout chip for arrival time, energy and/or photon counting measurements. *Nucl. Instrum. Methods Phys. Res. Sect. A-Accel. Spectrom. Dect. Assoc. Equ.*, *581*(1/2), 485–494.
7. Poikela, T., Plosila, J., Westerlund, T., & Campbell, M. (2014). Timepix3: a 65K channel hybrid pixel readout chip with simultaneous ToA/ToT and sparse readout. *JINST*, *9*(5), C05013.
8. Wong, W. S., Alozy, J., Ballabriga, R., Campbell, M., Kremastiotis, I., Llopart, X., Poikela, T., Sriskaran, V., Tlustos, L., & Turecek, D. (2020) Introducing Timepix2, a frame-based pixel detector readout ASIC measuring energy deposition and arrival time. *Radiat. Meas.*, *131*, 106230.
9. Bergmann, B., Burian, P., Manek, P., & Pospisiul, S. (2019). 3D reconstruction of particle tracks in a 2 mm thick CdTe hybrid pixel detector. *Eur. Phys. J. C*, *79*, 165. https://doi.org/10.1140/epjc/s10052-019-6673-z.
10. Zatko, B., Sagatova, A., Gal, N., Novak, A., Osvald, J., Bohacek, P., Polansky, S., Jakubek, J., & Kovacova, E. (2022) From a single silicon carbide detector to pixelated structure for radiation imaging camera. *JINST*, *17*, C12005.
11. Sagatova, A., Zatko, B., & Necas, V. (2018). From single GaAs detector to sensor for radiation imaging camera. *Appl. Surf. Sci.*, *461*(2), 3–9.
12. Zaťko, B., Zaprazny, Z., Jakubek, J., Sagatova, A., Bohacek, P., Sekacova, M., Korytar, D., Necas, V., Zemlicka, J., Mora, Y., & Pichotka, M. (2018) Imaging performance of Timepix detector based on semi-insulating GaAs. *JINST*, *13*, C01034.
13. Novak, A., Granja, C., Sagatova, A., Zach, V., Stursa, J., & Oancea, C. (2023) Spectral tracking of proton beams by the Timepix3 detector with GaAs, CdTe and Si sensors. *JINST*, *18*, C01022.
14. Jakubek, J., & Uher, J. (2009) Fast neutron detector based on TimePix pixel device with micrometer spatial resolution. In Proceedings of the 2009 IEEE Nuclear Science Symposium Conference Record (NSS/MIC), 24 October–1 November 2009, Orlando, FL, U.S.A. (pp. 1113–1116). DOI: 10.1109/NSSMIC.2009.5402420.
15. Bergmann, B., Nelson, R. O., O'Donnell, J. M., Pospisil, S., Solc, J., & Vykydal, Z. (2014). Time-of-flight measurement of fast neutrons with Timepix detectors. *JINST*, *9*, C05048.
16. Granja, C., Uhlar, R., Chuprakov, I., Alexa, P., Sansarbayar, E., Gledenov, Y. M., Poklop, D., Olsansky, V., Marek, L., Vuolo, M., & Pacik, J. (2023). Detection of fast neutrons with the pixel detector Timepix3. *JINST*, *18*, P01003.
17. Granja, C., Jakubek, J., Polansky, S., Zach, V., Krist, P., Chvatil, D., Stursa, J., Sommer, M., Plac, O., Kodaira, S., & Martisikova, M. (2018). Resolving power of pixel detector Timepix for wide-range electron, proton and ion detection. *Nucl. Instrum. Methods Phys. Res. Sect. A-Accel. Spectrom. Dect. Assoc. Equ.*, *908*, 60–71.
18. Sedlackova, K., Sagatova, A., Zatko, B., Necas, V., Solar, M., & Granja, C. (2016) MCNPX simulation of the silicon carbide semiconductor detector response to fast neutrons from D-T nuclear reaction. *Int. J. Modern Phys.-Conf. Ser.*, *44*, 1660226.
19. Simakov, S., Majerle, M., & Kostal, M. (2023) Recoil and charged particle energy spectra from the ^{nat}Si(n,x) reaction and the Si semiconductor detector response to the 14 MeV neutrons. *Radiat. Phys. Chem.*, *203*, 110624.
20. Jakubek, J., Granja, C., Hartmann, B., Jaekel, O., Martisikova, M., Opalka, L., & Pospisil, S. (2011). Selective detection of secondary particles and neutrons produced in ion beam therapy with 3D sensitive voxel detector. *JINST*, *6*, C12010.
21. Ziegler, J. F., Biersack, J. P., & Ziegler, M. D. (2008). *SRIM – The stopping and range of ions in matter*. NC, USA: Lulu Press Co.
22. Marek, L., Granja, C., Jakubek, J., Ingerle, J., Turecek, D., Vuolo, M., & Oancea, C. (2023). Data Processing Engine (DPE): Data Analysis Tool for Particle Tracking and Mixed Radiation Field Characterization with Pixel Detectors Timepix. *JINST*, prepared for publishing. https://arxiv.org/pdf/2310.15723v1.pdf.
23. Python Software Foundation. (2023 November). python™. [computer software]. Retrieved November 13, 2023, from https://www.python.org/.
24. Chadwick, M. B., Herman, M., Oblozinsky, P., Dunn, M. E., Danon, Y., Kahler, A. C., Smith, D. L., Pritychenko, B., Arbanas, G., Arcilla, R., Brewer, R., Brown, D. A., Capote, R., Carlson, A. D., Cho, Y. S., Derrien, H., Guber, K., Hale, G. M., Hoblit, S., Hollaway, S., Johnson, T. D., Kawano, T., Kiedrowski, B. C., Kim, H., Kunieda, S., Larson, N. M., Leal, L., Lestone, J. P., Little, R. C., McCutchan, E. A., MacFarlane, R. E., MacInnes, M., Mattoon, C. M., McKnight, R. D., Mughabghab, S. F., Nobre, G. P. A., Palmiotti, G., Palumbo, A., Pigni, M. T., Pronyaev, V. G., Sayer, R. O., Sonzogni, A. A., Summers, N. C., Talou, P., Thompson, I. J., Trkov, A., Vogt, R. L., van der Marck, S. C., Wallner, A., White, M. C., Wiarda, D., & Young, P. G. (2011). ENDF/B-VII.1 nuclear data for science and technology: Cross sections, covariances, fission product yields and decay data. *Nuclear Data Sheets*, *112*(12), 2887–2996. https://www.sciencedirect.com/science/article/pii/S009037521100113X.